JOC Article

Diastereochemically Controlled Porphyrin Dimer Formation on a DNA Duplex Scaffold

Masayuki Endo,* Mamoru Fujitsuka, and Tetsuro Majima*

The Institute of Scientific and Industrial Research, Osaka University, 8-1 Mihogaoka, Ibaraki, Osaka 567-0047, Japan

endo@sanken.osaka-u.ac.jp; majima@sanken.osaka-u.ac.jp

Received November 30, 2007

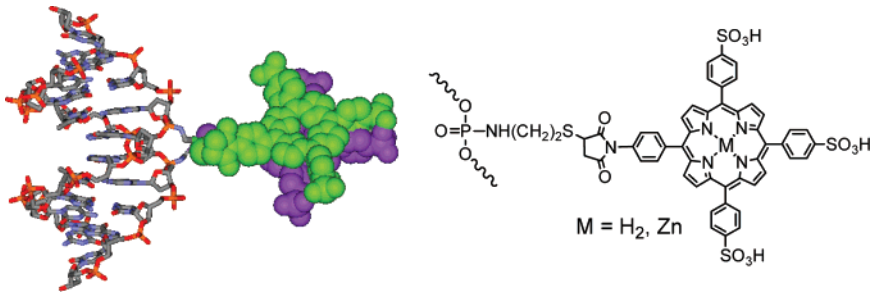

DNA-porphyrin conjugates were designed and synthesized for the preparation of the conformationally controlled porphyrin dimer structures constructed on a d(GCGTATACGC)$_2$. Porphyrin derivatives were introduced to the central TAT*p*A sequence where *p* represents the phosphoramidate for the attachment of the free-base porphyrin (FbP) and zinc-coordinated porphyrin (ZnP), which allows contact of the two porphyrins in the minor groove. The porphyrin dimers were characterized using CD, UV−vis, steady-state, and time-resolved fluorescence spectroscopies, indicating that the porphyrins form face-to-face conformations. Also the co-facial conformation was confirmed by comparison with spectra of the non-self-complementary duplex containing one porphyrin moiety. Introduction of zinc into porphyrin moiety destabilized the duplex formation. Two diastereomers showed different thermal stabilities and affected the conformations of porphyrin dimers. The temperature-dependent assembly and the conformational change of the porphyrin dimer on the duplex DNA were observed in the UV−vis spectra, indicating that the dynamic movement of the porphyrin dimer occurs on the duplex. The results indicate that the porphyrin dimers of DNA-FbP conjugates are overlapped clockwise and are located in the minor groove of the usual B-form DNA backbone. The interaction and conformation of two porphyrin moieties are controlled by the following three factors: (1) temperature change during and after formation of the duplex porphyrins at lower temperature; (2) diastereochemistry of the phosphoramidates where porphyrins are connected via a linker; and (3) zinc ion coordination that destabilizes the interaction of porphyrins as well duplex formation.

Introduction

Self-assembled chromophore systems are widely accepted for the construction of novel photochemical and electrochemical materials.[1−4] In these studies, the multichromophore system displayed completely different physical properties from the monomeric chromophore, therefore the defined arrangements and the number of chromophores are crucial issues for the final performance of the self-assembled system.[1−4] Porphyrin derivatives are some of the most attractive chromophores, which show not only a unique photochemical property such as the visible-light absorbing nature but also a physical property such as the formation of well-characterized assemblies under specific

* Address correspondence to this author. Phone: +81-6-6879-8495. Fax: +81-6-6879-8499.

(1) Hoeben, F. J.; Jonkheijm, P.; Meijer, E. W.; Schenning, A. P. H. *J. Chem. Rev.* **2005**, *105*, 1491−1546.

(2) Schenning, A. P. H. J.; Meijer, E. W. *Chem. Commun.* **2005**, 3245−3258.

(3) Hill, D. J.; Mio, M. J.; Prince, R. B.; Hughes, T. S.; Moore, J. S. *Chem. Rev.* **2001**, *101*, 3893−4011.

(4) Choi, M.; Yamazaki, T.; Yamazaki, I.; Aida, T. *Angew. Chem., Int. Ed.* **2004**, *43*, 150−158.

10.1021/jo7025004 CCC: $40.75
Published on Web 01/10/2008

conditions.[4−8] The anionic porphyrin, such as tetrakis(4-sulfonatophenyl)porphyrin, forms an H-aggregate under acidic conditions, and some counter cations also induce the H-aggregate formation.[6a−c] In addition, the photophysical properties can be easily changed by metal-coordination, in which heterogeneous combinations of porphyrin derivatives have been applied for energy-transfer and electron-transfer systems.[4,7,8] Also the cofacial Zn-porphyrin dimers have been investigated as a host for various guests such as bispyridine derivatives,[11] amino acids,[12] viologen,[13] and fullerene.[14] Controlled assembly of functional molecules using the support of DNA is a promising approach for the construction of structurally defined arrays of functional molecules.[15−16] Manganese porphyrin was first attached to an oligonucleotide for the preparation of site-selective DNA cleaving molecules.[17]Also porphyrin derivatives were conjugated to DNA for the investigation of DNA conformations and stabilizing the DNA structure.[17] Recently, branched DNA-porphyrin conjugates have been synthesized for the construction of DNA assemblies of multiple double helices and nanostructures.[19] By employing DNA as a scaffold to assemble chromophores, we intended to control the association and conformation of multiple porphyrins through the assembly of DNA strands under milder conditions.

In this study, we synthesized the DNA-porphyrin conjugates for the preparation of the conformationally controlled porphyrin dimer structures, and investigated the temperature-dependent assembly and the conformational change of the porphyrin dimer. To reduce the steric hindrance between duplex DNA and porphyrin moiety, the porphyrins were introduced to the phosphorus atom via a linker that is connected to the diastereochemically pure phosphoramidate for formation of the porphyrin dimer in the minor groove.[20] The orientations of the linkers on the phosphorus atom are completely different from each other; in the B-DNA structure, the R_p-configuration orients the linker toward the outer side of the double helix, while the S_p-configuration orients the linker toward the major groove.[20,21] This steric difference of diastereochemistry should affect the duplex-forming activity and porphyrin interaction. We characterized the interaction and conformational change of porphyrins on the duplex DNA scaffold by spectroscopic analysis and examined the effective formation of porphyrin dimer structures.

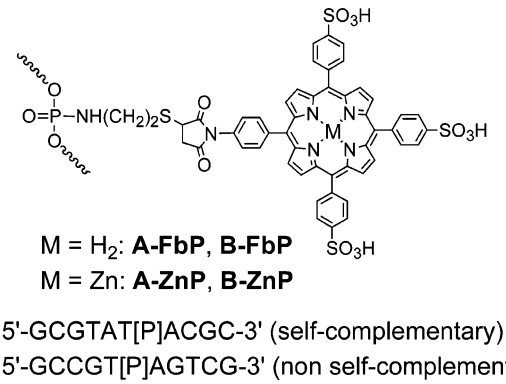

FIGURE 1. DNA-porphyrin conjugates and the sequences of self-complementary **1** and non-self-complementary **2** used in the experiment. A and B denote the diastereochemically pure isomers, which represent the faster and slower eluted products on a reversed-phase HPLC, respectively. FbP and ZnP represent free-base porphyrin and Zn-coordinated porphyrin, respectively.

Results and Discussion

Design And Synthesis of DNA-Porphyrin Conjugates. The self-complementary 10mer sequence 5′-GCGTATACGC-3′ (**1**) and the non-self-complementary 10mer sequence 5′-GCCGTAGTCG-3′ (**2**) were used as scaffolds for attachment of the porphyrin derivative (Figure 1).[20] The porphyrin derivatives were introduced to the internal phosphorus atoms at the specific position that is denoted as *p* in the sequences of 5′-GCGTAT-*p*ACGC-3′ (**1**) and 5′-GCCGT*p*AGTCG-3′ (**2**). Previous molecular modeling for the chemical interstrand cross-linking study of sequence **1** shows that these phosphorus atoms are located in the most proximal positions in the minor groove of the 10mer duplex.[20] The non-self-complementary sequence **2** is used as a reference for monomeric porphyrin on the duplex DNA for comparison with the dimeric porphyrins in the self-complementary sequence **1**.[21] The DNA oligomers containing diastereochemically regulated phosphoramidates were synthesized according to a previously reported procedure.[20,21] Two diaster-

(5) (a) Tsuda, A.; Osuka, A. *Science*, **2001**, *293*, 79−82. (b) Kim. D.; Osuka, A. *Acc. Chem. Res*. **2004**, *37*, 735−745. (c) Nakamura, Y.; Aratani, N.; Osuka, A. *Chem. Soc. Rev*. **2007**, *36*, 831−845.

(6) (a) Maiti, N. C.; Mazumdar, S.; Periasamy, N. *J. Phys. Chem. B* **1998**, *102*, 1528−1538. (b) Kano, K.; Fukuda, K.; Wakami, H.; Nishiyabu, R.; Pasternack, R. F. *J. Am. Chem. Soc*. **2000**, *122*, 7494−7502. (c) Schwab, A. D.; Smith, D. E.; Rich, C. S.; Young, E. R.; Smith, W. F.; de Paula, J. C. *J. Phys. Chem. B* **2003**, *107*, 11339−11345.

(7) (a) Holten, D.; Bocian, D. F.; Lindsey, J. S. *Acc. Chem. Res*. **2002**, *35*, 57−69. (b) Faure, S.; Stern, C.; Guilard, R.; Harvey, P. D. *J. Am. Chem. Soc.* **2004**, *126*, 1253−1261.

(8) (a) Osuka, A.; Nakajima, S.; Maruyama, K.; Mataga, N.; Asahi, T.; Yamazaki, I.; Nishimura, Y.; Ohno, T.; Nozaki, K. *J. Am. Chem. Soc.* **1993**, *115*, 4577−4589. (b) Osuka, A.; Tanabe, N.; Kawabata, S.; Yamazaki, I.; Nishimura, N. *J. Org. Chem*. **1995**, *60*, 7177−7185.

(9) Okada, S.; Segawa, H. *J. Am. Chem. Soc.* **2003**, *125*, 2792−2796.

(10) Wang, Z.; Medforth, C. J.; Shelnutt, J. A. *J. Am. Chem. Soc*. **2004**, *126*, 15954−15955.

(11) (a) Sugou, K.; Sasaki, K.; Kitajima, K.; Iwaki, T.; Kuroda, Y. *J. Am. Chem. Soc.* **2002**, *124*, 1182−1183. (b) Kobuke, Y.; Ogawa, K. *Bull. Chem. Soc. Jpn*. **2003**, *76*, 689−708. (c) Willson, G. S.; Anderson, H. L. *Chem. Commun.* **1999**, 1539−1540. (d) Screen, T. E. O.; Thorne, J. R. G.; Denning, R. G.; Bucknall, D. G.; Anderson, H. L. *J. Am. Chem. Soc.* **2002**, *124*, 9712−9703. (e) Twyman, L. J.; King, A. S. H. *Chem. Commun*. **2002**, 910−911. (f) Stulz, E.; Scott, S. M.; Bond, A. D.; Teat, S. J.; Sanders, J. K. M. *Chem. Eur. J*. **2003**, *9*, 6039−6048.

(12) (a) Guo, Y.-M.; Oike, H.; Aida, T. *J. Am. Chem. Soc*. **2004**, *126*, 716−717. (b) Proni, G.; Pescitelli, G.; Huang, X.; Nakanishi, K.; Berova, N. *J. Am. Chem. Soc*. **2003**, *125*, 12914−12927.

(13) Yagi, S.; Ezoe, M.; Yonekura, I.; Takagishi, T.; Nakazumi, H. *J. Am. Chem. Soc*. **2003**, *125*, 4068−4069.

(14) (a) Yamaguchi, T.; Ishii, N.; Tashiro, K.; Aida, T. *J. Am. Chem. Soc.* **2003**, *125*, 13934−13935. (b) Shoji, Y.; Tashiro, K.; Aida, T. *J. Am. Chem. Soc.* **2004**, *126*, 6570−6571. (c) Boyd, P. D. W.; Reed, C. A. *Acc. Chem. Res.* **2005**, *38*, 235−242.

(15) Nakamura, M.; Ohtoshi, Y.; Yamana, K. *Chem. Commun*. **2005**, 5163−5165.

(16) Mayer-Enthart, E.; Wagenknecht, H. A. *Angew. Chem., Int. Ed*. **2006**, *45*, 3372−3375.

(17) (a) Casas, C.; Lacey, C. J.; Meunier, B. *Bioconjugate Chem*. **1993**, *4*, 366−371. (b) Bigey, P.; Pratviel, G.; Meunier, B. *Nucleic Acids Res.* **1995**, *23*, 3894−3900. (c) Mestre, B.; Jakobs, A.; Pratviel, G.; Meunier, B. *Biochemistry* **1996**, *35*, 9140−9149.

(18) (a) Balaz, M.; Steinkruger, J. D.; Ellestad, G. A.; Berova, N. *Org. Lett.* **2005**, *7*, 5613−5616. (b) Balaz, M.; Holmes, A. E.; Benedetti, M.; Rodriguez, P. C.; Berova, N.; Nakanishi, K.; Proni, G. *J. Am. Chem. Soc*. **2005**, *127*, 4172−4173. (c) Balaz, M.; Li, B. C.; Jockusch, S.; Ellestad, G. A.; Berova, N. *Angew. Chem., Int. Ed*. **2006**, *45*, 3530−3533.

(19) (a) Endo, M.; Shiroyama, T.; Fujitsuka, M.; Majima, T. *J. Org. Chem*. **2005**, *70*, 7468−7472. (b) Endo, M.; Seeman, N. C.; Majima, T. *Angew. Chem., Int. Ed*. **2005**, *44*, 5074−5077.

(20) Endo, M.; Majima, T. *Org. Biomol. Chem.* **2005**, *3*, 3476−3478.

(21) (a) Endo, M.; Majima, T. *J. Am. Chem. Soc*. **2003**, *125*, 13654−13655. (b) Endo, M.; Majima, T. *Angew. Chem., Int. Ed*. **2003**, *42*, 5744−5747. (c) Endo, M.; Uegaki, S.; Majima, T. *Chem. Commun*. **2005**, 3153−3155.

TABLE 1. Melting Temperatures of DNA and Porphyrin Derivatives of the DNA-Porphyrin Conjugates[a]

	DNA region		porphyrin region	
DNA	T_m/°C	ΔT_m/°C	T_m/°C	ΔT_m/°C
1A-FbP	46.3	−3.2	43.2	−3.1
1B-FbP	50.3	+0.8	47.7	−2.6
2A-FbP	38.3	−12.9		
2B-FbP	41.1	−10.1		
1A-ZnP	nd		22.2	
1B-ZnP	38.9	−10.6	34.7	−4.2
2A-ZnP	38.1	−14.1		
2B-ZnP	42.7	−8.5		

[a] Dissociation of DNA was monitored at 260 nm, and those of FbP and ZnP were monitored at 420 and 427 nm, respectively. T_m values of native **1** and **2** were 49.5 and 51.2 °C, respectively. nd, not determined. ΔT_m in the DNA region represents the difference from the T_m of unmodified duplex. ΔT_m in the porphyrin region represents the difference from the T_m of the corresponding DNA.

eomers denoted as A and B correspond to the faster eluted peaks and slower ones on a reversed-phase HPLC, respectively (Figure S1, Supporting Information). Porphyrin derivatives, FbP-maleimide **3** and ZnP-maleimide **4**, were synthesized according to Scheme S1 (Supporting Information). We introduced three sulfonate groups for solubility for water and the maleimide group for maleimido-thiol coupling. The primary amine of the tetrabutylammomium salt of the starting porphyin[22] was converted into maleimide using maleic anhydride in acetonitrile and then with acetic anhydride and sodium bicarbonate to give the FbP-maleimide **3** (90% yield). Introduction of zinc ion to **3** using zinc acetate gave ZnP-maleimide **4** (95% yield). The oligonucleotides containing a diastereochemically pure phosphoramidate were treated with DTT for the preparation of thiol-tethered DNA (DNA-SH). DNA-porphyrin conjugates were prepared by coupling the DNA-SH with excess FbP-maleimide **3** or ZnP-maleimide **4**, purified by HPLC (Figure S2, Supporting Information), and identified using MALDI-TOF mass spectroscopy (Figure S3, Supporting Information).

Thermal Stabilities of Porphyrin Dimer and Duplex DNA. The stabilities of the duplexes were examined by melting temperature (T_m) measurements (Table 1). We measured the thermal denaturation profiles of the DNA region (260 nm) and the porphyrin region (420 and 427 nm for FbP and ZnP, respectively) (Figure 2). DNA-porphyrin derivatives showed typical melting curves of denaturation of duplex DNA. In the cases of the DNA-FbP conjugates, porphyrin moieties did not work for the significant stabilization of the duplex, suggesting that the negative charge repulsion between two porphyrin derivatives may lead to the destabilization of the duplex. In addition, the stereochemical effects of the phosphoramidates were observed, and the complexes containing B-diastereomers (**1B-FbP**) were thermally more stable than those with A-diastereomers.[20−21] In the cases of the DNA−ZnP conjugates, **1A-ZnP** showed a significantly different behavior as compared to DNA−FbP conjugates. The melting profile of the DNA region of **1A-ZnP** did not show a stable duplex even at lower temperature (Figure 2C). In contrast, although the stability of **1B-ZnP** decreased as compared to that of **1B-FbP**, **1B-ZnP** formed a stable duplex at lower temperature as shown in the melting profile (Figure 2D). Because the zinc is located out of the porphyrin plane and a water molecule occupies an axial position of the zinc ion, coordination of zinc prevents the porphyrin aggregation as compared to that of FbP.[21,22] Therefore, the ZnP negatively affected not only the porphyrin interaction, but also the stability of duplex formation.

In the melting profiles monitored by the absorption change in the porphyrin derivatives, the changes in the porphyrin regions showed the dynamic movements of the porphyrin dimer. The absorption curves of the porphyrin parts showed slightly lower values than the melting curve of duplex DNA depending on the temperature (Figure 2). These results indicate that the porphyrins dissociate before dissociation of the DNA duplex.

The results of the stabilities of DNA-porphyrin duplexes also showed the clear diastereomer effect. The duplexes of the B-diastereomers were more stable than those of the A-diastereomers, similar to the results of the other diastereomers previously studied.[20,21] Because the A- and B-diastereomers used in this experiment have been estimated as the S_p- and R_p-configurations, respectively,[20] the tether of the R_p-configuration directs to the minor groove, which is advantageous for assembling the chromophores in the minor groove. Therefore, the B-diastereomers in both FbP and ZnP conjugates allowed contact of two porphyrin moieties with smaller stress as compared to the A-diastereomers. Zn coordination in the A-diastereomer significantly decreased the stability of the duplex, and the ZnP dimer formation on the B-diastereomer is also structurally more favorable than that on the A-diastereomer.

Absorption Spectral Change of Porphyrin Moieties in the Duplex DNA. To investigate the interaction of the two porphyrins, the UV−vis spectral changes of DNA-porphyrin conjugates were monitored by increasing the temperature after annealing of the DNA-porphyrin conjugates (Figure 2). In the cases of **1A-FbP** and **1B-FbP**, the wavelength of the maximum absorption peak of the Soret band was 412 nm at 10 °C (Figure 3, parts A and B). By increasing the temperature, the peaks gradually shifted to a longer wavelength (420 nm at 70 °C) with increasing absorbance of the peaks. The shapes of the peaks significantly changed around 40−60 °C, which corresponds to the dissociation of the DNA strands. As compared to the dissociated state of DNA at 70 °C and the duplex state below 30 °C, the peaks shifted to a shorter wavelength by 8 nm accompanying broadening of the peaks by decreasing the temperature during the duplex formation. This result indicates that the transition dipoles of the two porphyrins favorably overlap to form a face-to-face conformation such as an H-like aggregate.[6] At lower temperature (10−20 °C), the Soret band of the porphyrin shifted from 412 to 414 nm without significantly changing the absorbance, indicating the conformational change of porphyrin dimer on duplex DNA during association of the porphyrin dimer. In spite of the difference in the configuration of the phorphoramidate, the spectra of the Soret bands of both diastereomers were quite similar at 10 °C, indicating that the linkers are flexible enough to allow two porphyrins to form a thermally favorable conformation.

For the control experiments, the temperature-dependent spectral changes of the non-self-complementary DNA-porphyrin conjugates **2-FbP** (both A- and B-diastereomers) with its complementary strand were examined (Figure S6, Supporting Information). The absorbance of the Soret band decreased by decreasing the temperature accompanying the long wavelength shift by 2−3 nm under the same conditions, indicating that the

(22) Kruper, W. J., Jr.; Chamberlin, T. A.; Kochanny, M. *J. Org. Chem.* **1989**, *54*, 2753−2756.
(23) Pasternack, R. F.; Francesconi, L.; Raff, D.; Spiro, E. *Inorg. Chem.* **1973**, *12*, 2606−2611.
(24) Hoard, J. L. *Science* **1971**, *174*, 1295−1302.

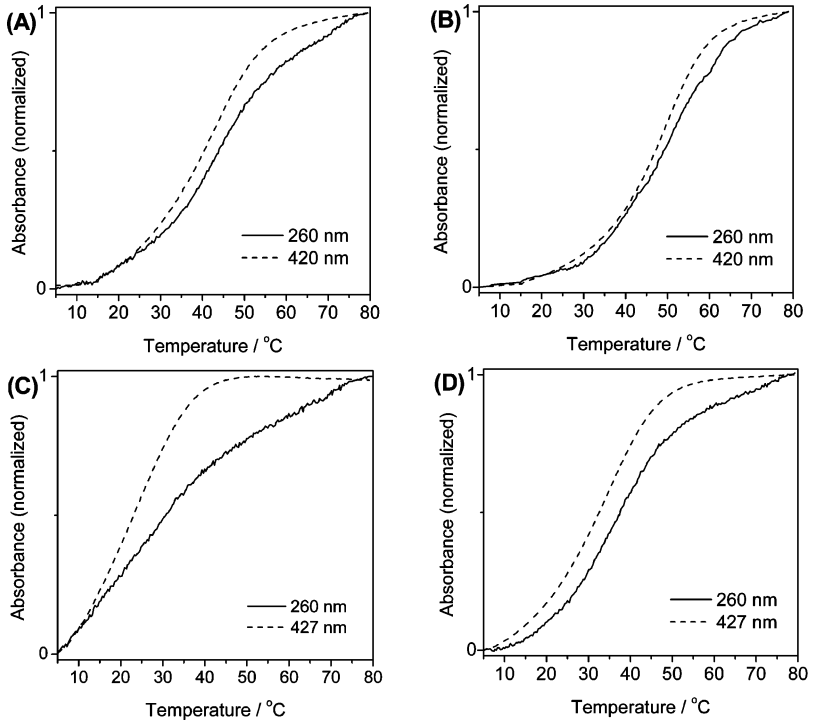

FIGURE 2. Melting profiles of the DNA-porphyrin conjugates **1A-FbP** (A), **1B-FbP** (B), **1A-ZnP** (C), and **1B-ZnP** (D). Solid lines and dashed ones represent the absorbance changes monitored at 260 nm for the absorbance of DNA and at 420 and 427 nm for those of FbP and ZnP derivative, respectively.

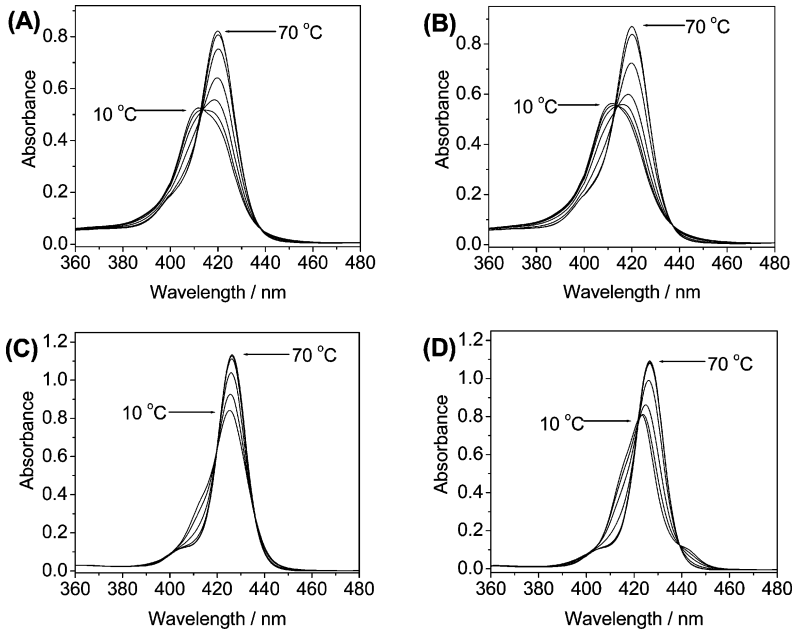

FIGURE 3. Temperature-dependent spectral changes of DNA-porphyrin conjugates: free-base porphyrin derivatives **1A-FbP** (A) and **1B-FbP** (B); Zn-porphyrin derivatives **1A-ZnP** (C) and **1B-ZnP** (D). The spectral changes were monitored every 10 °C by heating from 10 to 70 °C.

single FbP attached to the DNA may intercalate into the duplex DNA. In addition, free FbP-maleimide **3** formed the different H-aggregates as compared to those of the **1-FbP** conjugates both in the absence and in the presence of duplex DNA (Figure S7, Supporting Information). The clearly different behaviors of the single porphyrin in the **2-FbP** duplexes from the double porphyrins in the **1-FbP** duplexes confirm that the porphyrins in the **1-FbP** duplexes favorably form face-to-face conformations.

We also examined the spectral changes of DNA-ZnP conjugates. The absorption of the Soret band of **1A-ZnP** continuously decreased at lower temperature, and the peak shift was very small (Figure 2C). In contrast, the Soret band of **1B-ZnP** shifted to a shorter wavelength from 427 (70 °C) to 423 nm (10 °C) accompanying the decrease in the absorbance of the peak by lowering the temperature (Figure 3D), which was similar to that of the case of DNA-FbP conjugates described above. At lower temperature (10−20 °C), the peak shifted from

TABLE 2. Fluorescence Properties of DNA-Porphyrin Conjugates[a]

DNA	emission/nm λ_{ex} = 412 nm	emission/nm λ_{ex} = 420 nm	τ/ns	DNA	emission/nm λ_{ex} = 423 nm	emission/nm λ_{ex} = 427 nm	τ/ns
1A-FbP	660, 724	657, 719	12.6	**1A-ZnP**	607, 656	607, 656	2.4
1B-FbP	662, 728	660, 725	11.5	**1B-ZnP**	608, 658	608, 658	2.4
2A-FbP	653, 715	654, 717	11.4	**2A-ZnP**	605, 654	605, 654	2.3
2B-FbP	653, 714	653, 716	11.3	**2B-ZnP**	608, 658	608, 658	2.3

[a] Measurements were carried out in a solution containing 2.0 μM DNA−porphyrin conjugates, 10 mM phosphate buffer (pH 7.0), and 1.0 M NaCl. Duplexes of DNA−porphyrin conjugates **2** contained 1.0 μM DNA−porphyrin conjugates and the complementary strand.

424 to 423 nm with a small change of the absorption, indicating that the conformational change of the ZnP dimer proceeds at lower temperature. We also examined the temperature-dependent spectral changes of **2-ZnP** with the complementary strand. The spectral changes of the Soret bands in the **2-ZnP**s were modest as compared to those in the **1-ZnP**s under the same condition (Figure S6, Supporting Information). Also the free ZnP-maleimide **4** did not form any aggregates in the absence and presence of duplex DNA (Figure S7, Supporting Information). These results indicate that the two ZnPs in the **1B-ZnP** can form the overlapped conformations, and the formation of the porphyrin dimers in the **1-ZnP** is very sensitive to the diastereochemistry of the phosphoramidates.

Fluorescence Properties of DNA-Porphyrin Conjugates. Fluorescence spectra of the DNA-porphyrin conjugates in the DNA were investigated (Table 2). The peaks in all the emission spectra excited at the Soret band region have features of typical porphyrin derivatives (Figure S8, Supporting Information). In the cases of the DNA-FbP conjugates, the emission peaks excited at the aggregation band in the Soret band (412 nm) largely shifted to longer wavelengths (7−14 nm) as compared to those of the **2-FbP** duplexes, indicating the strong coupling of the two porphyrin moieties. These peaks were also shifted to longer wavelengths (2−5 nm) as compared to those excited at the monomeric FbP Soret band (420 nm) of the **1-FbP**. In addition, the difference in the peaks of the two diastereomers was observed. All the emission peaks of the **1B-FbP** showed longer wavelengths (2−6 nm) than those of the **1A-FbP**, indicating that the B-diastereomer is advantageous to place the porphyins in a favorable overlapped conformation. Time-resolved fluorescence spectra were measured for the DNA-porphyrin conjugates. The decay curves of both the DNA-porphyrin derivatives can be fitted to single exponential, meaning that the two porphyrins form a single conformation. Fluorescence lifetimes of **1A-FbP** and **1B-FbP** were different, and also different from those of the monomeric porphyrin on the duplex.

For the DNA-ZnP conjugates, 423 (dimeric) and 427 nm (monomeric) were used for the excitation. No peak shifts were observed in the spectra of **1A-ZnP** and **1B-ZnP** with these two excitation wavelengths, suggesting the smaller coupling of ZnPs on the duplex DNA. Different emission peaks of the monomeric **2A-ZnP** from those of **1A-ZnP** were observed. This difference may originate from the interaction between DNA and ZnP in **2A-ZnP** observed in the temperature-dependent UV/vis spectral changes (Figure S6C, Supporting Information).

Conformations of Porphyrin Dimers Investigated by CD Spectroscopy. The interactions of the porphyrin moieties and DNA backbone structures were examined by circular dichroism (CD) spectroscopy (Figure 4). We investigated the characteristic CD bands of both DNA duplex and porphyrin moieties. At first, the backbones of the DNA structures were characterized. In the

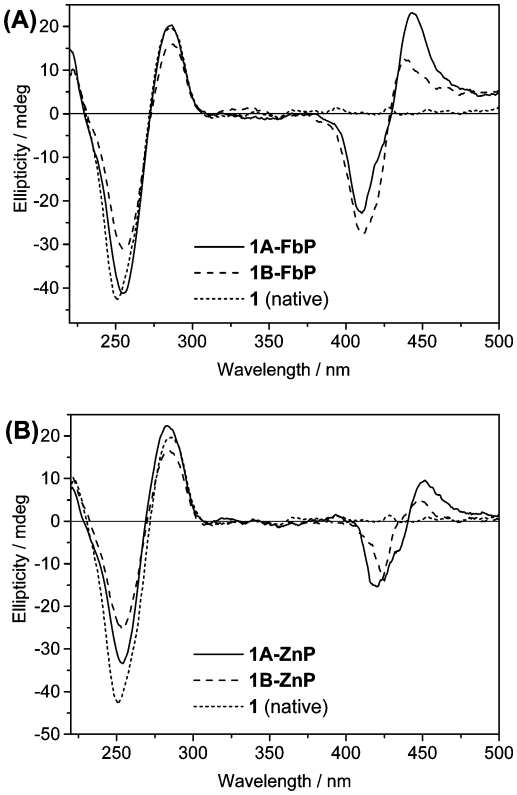

FIGURE 4. CD spectra of the DNA-porphyrin conjugates: (A) **1A-FbP** (solid line) and **1B-FbP** (broken line); (B) **1A-ZnP** (solid line) and **1B-ZnP** (broken line). CD spectrum of the native 10mer duplex **1** (native) is also shown as a reference (dotted line).

DNA structure of the **1A-FbP**, the intensities of the negative and positive bands (260 and 280 nm, respectively), which are characteristic for a double helix structure, were similar to those of the native duplex structures.[25] Both DNA structures containing two DNA-porphyrin units with the A- or B-diastereomers formed characteristic B-form double helix structures.[25]

We next examined the induced CD bands in the porphyrin regions. CD spectra of **2-FbP** duplexes were examined as references, where single porphyrin was located on duplex DNA. In the CD spectra of monomeric porphyrins in **2-FbP** duplexes, the positive induced CD bands originating from the Soret band of the porphyrin derivatives were observed around 400−450 nm (Figure S9, Supporting Information). In contrast, the strong negative and positive induced CD bands were observed in the spectra of both **1-FbP** duplexes. **1A-FbP** and **1B-FbP** showed different induced CD bands in the porphyrin region. In the case

(25) Johnson, W. C. *Circular Dichroism, Principles and Applications*; Berova, N., Nakanishi, K., Woody, R.W., Eds.; Wiley-VCH: New York, 2000; pp 703−718.

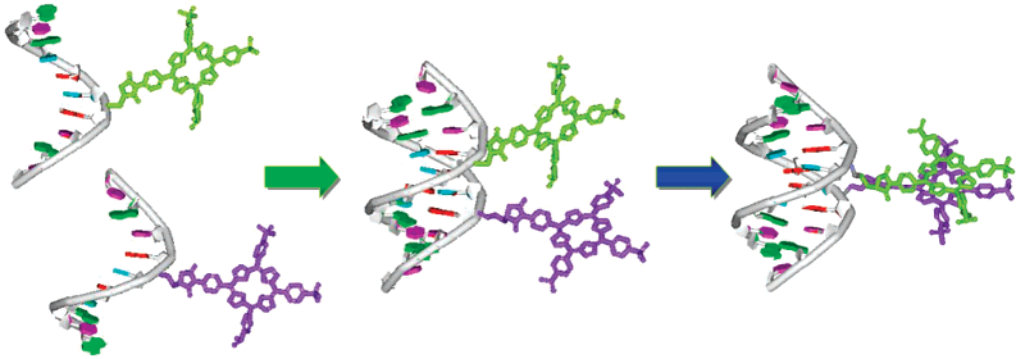

FIGURE 5. Interaction of DNA and porphyrin moieties during self-assembly by decreasing the temperature. DNA duplex formation in the first step followed by porphyrin H-like aggregate formation in the second step.

of **1A-FbP**, strong negative and positive bands appeared at 410 and 443 nm, respectively. Strong negative and weaker positive bands were observed in **1B-FbP** at 410 and 438 nm, respectively. The appearance of positive and negative CD bands indicates the excitonic coupling between two porphyrin chromophores.[18,26] The differences in the patterns of the CD bands of the porphyrin region between the A- and B-diastereomer are attributed to the conformation of the overlapped porphyrins, which originate from the configurations of phosphoramidates where these porphyrins are attached. The observed positive CD exciton couplet in the spectrum indicates the clockwise overlap of the transition dipoles of two porphyrins on the duplex DNA.[26]

In the cases of the ZnP-attached DNA, excitonic couplings were also observed, and the band shapes between **1A-ZnP** and **1B-ZnP** were different. Excitonic couplings of the ZnP dimers were much weaker than those of the free base porphyrin dimers, because the zinc coordination to the porphyrin weakens the interaction of ZnPs as compared to the interactions of FbPs.[23,24] These results suggest that the two ZnPs may not form fully overlapped dimer structures on these DNA duplex scaffolds.

Conclusions

We have designed and synthesized the DNA-porphyrin conjugates and characterized the interaction of the porphyrins on the duplex. Excitonic coupling of the porphyrins observed in the spectra of dimeric DNA-FbP conjugates shows that the porphyrins preferentially form a face-to-face conformation. Also the face-to-face conformation was confirmed by comparison with spectra of the non-self-complementary duplex with a monomeric porphyrin. Based on the results of the spectroscopic data, the structure of DNA-FbP conjugates **1A-FbP** is shown in the abstract figure, and the overall interactions of the DNA and porphyrin moieties are described as an illustration in Figure 5. Two porphyrins overlapped clockwise are located in the minor groove, which are connected to the phosphoramidate with the R_p-configuration in the usual B-form DNA backbone. During the porphyrin dimer formation process by decreasing the temperature, the duplex formation occurs first, and then the two porphyrins approach to form a dimer structure. By further decreasing the temperature, the porphyrin dimer changes the conformation on the duplex DNA to form the thermally favorable face-to-face conformation in the cases of the DNA-FbP conjugates. Although the ZnPs also formed the dimer structures on the duplexes, overlap of two ZnPs is small, and ZnP negatively affected the stabilities of duplexes. Diastereochemistry of the phosphoramidate was also a key factor for the porphyrin dimer formations and the duplex stabilities. Using the selective assembly of the duplex DNA, the heterogeneous porphyrins and other chromophores can be introduced in the minor groove of the DNA. These DNA-chromophore conjugates can be expanded for the construction of the DNA-assisted and structurally controlled multichrophore system.

Experimental Section

Synthesis of DNA-Porphyrin Conjugates. A disulfide tether was introduced via a phosphoramidate linkage in the center of the 10-mer single-strand DNA according to a previously reported method.[19−21] Two adjacent diastereomer peaks (A- and B-diastereomers) were separated by reversed-phase HPLC [linear gradient using 2−8% acetonitrile/water (20 min) containing 50 mM ammonium formate, Nacalai Cosmosil C18 reversed-phase column (7.5 × 150 mm), 2.0 mL/min, 260 nm] (Figure S1, Supporting Information). The purified diastereochemically pure oligonucleotide (10 nmol) was reduced in a solution containing 50 mM Tris-HCl (pH 8.0) and 10 mM DTT at 50 °C for 30 min. The thiol-attached DNA (DNA-SH) was purified by reversed-phase HPLC (the same conditions as described above). The DNA-SH was treated with a 0.1 mM acetonitrile solution of free base porphyrin-maleimide **3** or Zn-porphyrin maleimide **4** in 50 mM ammonium formate (pH 6.5) at 30 °C for 2 h. DNA-porphyrin conjugates were purified by HPLC [the same conditions as described above except for a linear gradient using 2−50% acetonitrile/water (20 min)], and finally lyophilized. MALDI-TOF MS (negative): **1-FbP** calcd 4036.1 [M − H]$^-$, found: **1A-FbP**, 4037.7; **1B-FbP**, 4036.7. **1-ZnP** calcd 4099.5 [M − H]$^-$, found: **1A-ZnP**, 4099.3; **1B-ZnP**, 4100.3.

UV−Vis Spectroscopy. Temperature-dependent absorption spectra were obtained on a UV−vis spectorophotometer equipped with a temperature controller. A solution containing 2.0 μM DNA-porphyrin conjugate, 10 mM phosphate buffer (pH 7.0), and 1.0 M NaCl was heated at 85 °C in a quartz cell, and then slowly cooled to 4 °C. Spectra were obtained every 10 °C by heating from 10 to 70 °C. Using the same solution, thermal denaturation profiles were obtained. The absorption changes in the DNA region were monitored at 260 nm, and those of the FbP and ZnP were monitored at 420 and 427 nm, respectively. Temperature was increased at a rate of 1.0 deg/min. The first derivative calculated from the melting profile was used to determine the T_m value.

Fluorescence Spectroscopy. Measurements were carried out at 20 °C in a solution containing 2.0 μM DNA-porphyrin conjugate, 10 mM phosphate buffer (pH 7.0), and 1.0 M NaCl.

(26) Berova, N.; Nakanishi, K. *Circular Dichroism, Principles and Applications*; Berova, N., Nakanishi, K., Woody, R.W., Eds.; Wiley-VCH: New York, 2000; pp 337−382.

Circular Dichroism (CD) Spectroscopy. Measurements were carried out at 20 °C in a solution containing 10 μM DNA-porphyrin conjugate, 10 mM phosphate buffer (pH 7.0), and 1.0 M NaCl using a quartz cell with a 2 mm path length.

Time-Resolved Fluorescence Spectroscopy. Fluorescence decays were acquired by the single photon counting method using a streak scope (Hamamatsu Photonics, C4334-01). Samples were excited with a second harmonic generation (420 nm) of a Ti^{-}: sapphire laser (Spectra Physics, Tsunami 3941-M1BB, fwhm 100 fs). Measurements were carried out at 23 °C in a solution containing 2.0 μM DNA-porphyrin conjugate, 10 mM phosphate buffer (pH 7.0), and 1.0 M NaCl.

Acknowledgment. This work has been partly supported by a Grant-in-Aid for Scientific Research (Project 17105005, Priority Area (417), 21st Century COE Research, and others) from the Ministry of Education, Culture, Sports, Science and Technology (MEXT) ofthe Japanese Government.

Supporting Information Available: Characterization of DNA-porphyrin conjugates. This material is available free of charge via the Internet at http://pubs.acs.org.

JO7025004